Human Body Shadowing Characterization for 60 GHz Indoor Short-Range Wireless Links

Petros Karadimas, *Member, IEEE*, Ben Allen, *Senior Member, IEEE* and Peter Smith, *Senior Member, IEEE*

***Abstract*—We statistically characterize received signal power variations in the time domain caused by human activity affecting *60GHz* indoor short-range wireless links. Our approach is based on propagation measurements in indoor environments considering human activity intercepting the line-of-sight (LOS) path. It has been previously shown that the ensemble of received power levels in *dB* scale cannot be modeled by a Gaussian distribution, as is the case for spatial shadowing variations. In this letter, we present a theoretical stochastic approach showing that received power variations can follow a Gaussian statistical model when considered within the time intervals of similar shadowing processes. Our model is shown to have good comparison with experimental data.**

***Index Terms*—*60GHz* wireless communications, human body shadowing, indoor propagation.**

I. Introduction

60GHz wireless technology has arisen as an exciting opportunity for supporting multi-gigabit per second (Gbps) communication systems [1]. For indoor short-range wireless communications, this technology has been standardized by the IEEE, i.e., IEEE 802.15.3c [2] and IEEE 802.11ad [3] standards. These standards are extensions of the existing IEEE 802.15.3 and IEEE 802.11 standards, respectively.

60GHz short-range wireless transmissions are susceptible to shadowing loss due to the inherent human activity obstructing the line-of-sight (LOS) path [4]-[8]. Shadowing loss is further influenced because of the utilization of directional antennas to overcome the increased path loss and effects of multipath propagation that are present at these frequencies [9]. It is well-known that spatial shadowing variations in *dB* scale are modeled by a Gaussian distribution [10], [11]. However, there is not a rigorous statistical description in the published literature for the temporal variability of shadowing of LOS paths due to human activity. This seems surprising due to the significant impact human body shadowing has on *60GHz* wireless links. Very recent advances based on measurements and simulations revealed that knowledge of human body shadowing is essential to estimate the performance [12] and also design of spatial diversity schemes to mitigate the performance reduction [13].

Statistical investigations of shadowing events (i.e., shadowing probabilities and shadowing duration) due to human activity in indoor environments were presented in [4]. An empirical cumulative distribution function (CDF) of power loss due to human shadowing was presented in [5], but without any further statistical analysis. In [6], it was shown that the whole ensemble of power levels when human shadowing occurs cannot be modeled by a Gaussian distribution. In [7], the shadowing spatial variations were separated from the shadowing temporal variations due to human activity. In [8], it was considered that human activity influences the first and second order reflections, whereas the LOS path remained unobstructed. Gaussian and mixture Gaussian distributions were used to model second and combined first/second order reflections, respectively. A complete statistical description of received power levels due to the shadowed LOS path was not presented in [4]-[8]. The latter forms the subject of this letter.

We present received power measurements in the time domain using a system that captures and stores power in the *60GHz* band. From the collected measurements, we extend the analysis in [6] showing that a Gaussian distribution can be a good fit for the power levels in *dB* scale only within the time intervals of similar shadowing processes. This is different from the case of spatial variability of shadowing, where the whole ensemble of received power levels in *dB* scale follows a Gaussian distribution, as in [10] and [11]. Our analysis is based on the development of a stochastic modeling approach, which extends that in [10] to account for time-dependent shadowing variations.

II. Measurement Set-Up

Our measurement system is based on a VμBIQ *60GHz* wireless development system [14]. The transmitting system consists of:

a. RF sinusoidal signal generator,

b. I/Q power splitter and two *0°/180°* power splitters to generate the differential I/Q inputs to the transmitter,

c. VμBIQ up-converter *60GHz* synthesizer,

d. transmitting antenna.

The receiving system consists of:

a. receiving antenna,

b. VμBIQ down-converter *60GHz* synthesizer,

c. I/Q power combiner and two *0°/180°* power combiners to generate the differential I/Q outputs from the receiver,

d. band-pass filter to reduce the noise power,

Manuscript received February 15, 2013.

Petros Karadimas and Ben Allen are with the Centre for Wireless Research, University of Bedfordshire, Luton, LU1 3JU, UK, (e-mail: Petros.Karadimas@beds.ac.uk, Ben.Allen@beds.ac.uk).

Peter Smith is with the Department of Electrical and Computer Engineering, University of Canterbury, Christchurch, New Zealand (e-mail: Peter.Smith@canterbury.ac.nz).

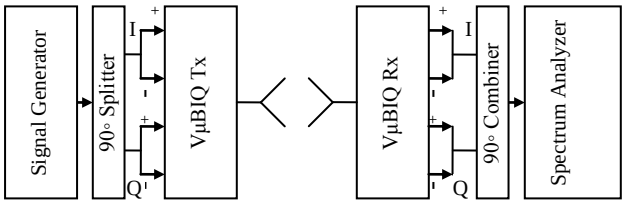

Fig. 1. Block diagram of the measurement system.

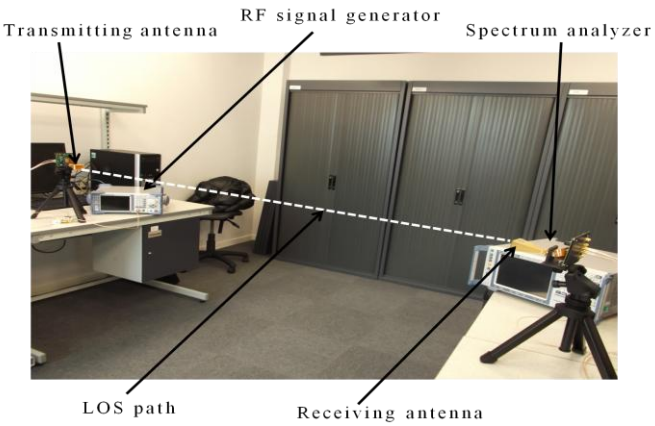

Fig. 2. Measurement system and the indoor propagation environment.

e. the spectrum analyzer,

f. computer to log the measured data.

A block diagram of the measurement system is shown in Fig. 1. The receiving and transmitting horn antennas are vertically polarized and have *24dBi* maximum gains and a *3dB* beamwidth of *12* and *11* degrees in the H- and E-planes, respectively. The RF sinusoidal signal generator is set to *800MHz* and *-10dBm*. The VμBIQ transmitter up-converts the frequency to the *60GHz* band, incorporates a digital frequency synthesizer and power amplifier and has a *1GHz* baseband input bandwidth. At the VμBIQ receiver, the received signal is down-converted and sent to the spectrum analyzer. Finally, the raw power measurements are then stored on the computer. To obtain time domain power measurements, the frequency span of the spectrum analyzer is set to *0Hz*. By setting the sweep time to *5sec*, the measured data are stored into blocks of *5sec*.

Eight measurement sets have been collected, categorized within two representative categories for human body shadowing in indoor short-range wireless communications. The first category contains three measurement sets where realistic mobility of two people (with a speed of about *1m/sec*) intercepted the LOS path in an ad-hoc manner. The second category contains five measurement sets where a human body remains static between the antennas. The distance between the transmitting and receiving antennas was *2.5m* and *2m* for the first and second category, respectively. Human bodies are of regular pattern in terms of size, weight and clothing and blockage is mainly due to the upper parts of body. The considered scenarios are adequate for the purpose of our analysis, i.e., to statistically characterize shadowing both theoretically and through measurements when human activity occurs. Fig. 2 shows a photograph of the indoor propagation environment together with the components of our measurement system.

III. Statistical Analysis and Results

The received power under the presence of human activity between the transmitting and receiving antennas is given by [7]

$$P_r(t) = P_t + G_t + G_r - PL - PL_h(t) \tag{1}$$

where t is the time, $P_r(t)$ the received power, P_t the transmitted power, G_r the receiving antenna gain, G_t the transmitting antenna gain, PL the distance dependent path loss and $PL_h(t)$ the time dependent shadowing loss due to human activity. Apart from t, all other quantities in equation (1) are expressed in a *dB* scale. As the wireless links are point-to-point and the distance d between the transmitting and receiving antennas is kept fixed, PL will be constant representing the free space path loss. Thus, assuming the absence of any secondary rays due to the use of very directional antennas, $PL = 10\log_{10}[\lambda^2/(4\pi d)^2]$, where λ is the carrier wavelength. Due to the random time varying nature of people's mobility, $PL_h(t)$ will be a time varying stochastic process, thus making $P_r(t)$ a time varying stochastic process. It is evident that the statistics and temporal evolution of $P_r(t)$ will be similar to those of $PL_h(t)$.

Extending the analysis in [10], which uses an additive model [15] as a basis for analyzing and modeling shadowing, we can show that $P_r(t)$ in a *dB* scale follows a Gaussian distribution within the time intervals of similar shadowing processes, i.e. when shadowing arises from the same effect, for example, realistic mobility of two people as in the first category, or static bodies between the antennas as in the second category. More specifically, we express the received narrowband signal in complex baseband form as a summation of homogeneous time varying plane waves, i.e., as an additive model [15]

$$h(t) = \sum_{l=1}^{L} a_l \exp(j2\pi v_{d,l} t) \tag{2}$$

where a_l is the complex amplitude, i.e., $a_l = |a_l|\exp(j\phi_l)$ and $v_{d,l}$ the Doppler frequency of the lth plane wave induced by human motion. a_l incorporates the impact of antenna patterns on the lth plane wave [10], [15]. The number of plane waves in equation (2) is infinite considering scattering patterns of human bodies similar to [16]. In our case, it is evident that temporal variability is the only variability, as both the transmitting and receiving antennas are static. Analogous to the definition of local area (LA) [17], we can define the restricted time interval (RTI) as the maximum time interval T, where $|a_l|$ and $v_{d,l}$ are constants. Moreover, if ϕ_l are uncorrelated and uniformly distributed in $[0, 2\pi]$, then $h(t)$

will be a wide sense stationary (WSS) process with respect to time [17][1]. In this case, the mean received power within T will be [17][2]

$$P_r = E\left[\left|h(t)\right|^2\right] = \sum_{l=1}^{L}\left|a_l\right|^2 \quad (3).$$

where $E[.]$ is the expectation operator.

Considering equation (3) in different RTIs, the power of the plane waves, and consequently P_r, change with time, i.e., P_r becomes $P_r(t)$. Such variations are attributed to random human activity causing different scattering cross sections to be illuminated by the transmitting antenna and seen by the receiving antenna. Thus, $P_r(t)$ will be a time varying stochastic process with realizations $\{P_{r,1}(t), P_{r,2}(t), ...\}$. Analogous to the definition of extended LA (ELA) [10], we define the extended RTI (ERTI) as the maximum time interval T_e, comprising of several RTIs, where the plane wave powers (i.e., $\left|a_l\right|^2$) are stationary random variables. The practical implication of such a definition is that within T_e, the received signal is influenced by the same shadowing processes. In fact, T_e is the duration of shadowing events, which depends on the type of mobility (static bodies, slow people mobility, etc) and the number of people moving between the antennas [4]. Thus, assuming that the plane wave powers are statistically independent random variables and adopting the main result presented in [10], we conclude that $P_r(t)$ in *dB* scale is Gaussian distributed within T_e and when the number of plane waves is infinite, i.e., $P_r(t)$ is a Gaussian stochastic process when $L \to \infty$. However, with a large number of plane waves, which is the practical case, $P_r(t)$ in *dB* scale is approximately Gaussian distributed. As with [10], such a result holds for any frequency of operation, type and number of scatterers, antenna patterns and polarizations. However, in this letter our focus is on the *60GHz* band when using directional antennas and shadowing occurs due to human activity. From the above analysis, it is evident why the whole ensemble of power levels cannot follow a Gaussian distribution, as was shown in [6].

Fig. 3 shows representative examples of the time-domain, normalized to LOS, received power (LOS power is normalized to *0dBm*) for each shadowing category. Each of the two categories accounts for a different shadowing process. The first category accounts for human body shadowing due to slow mobility of two individuals (with a speed of about *1m/sec*). In total, three realization sets have been obtained in the first category, see [6]. The second category accounts for human body shadowing due to static bodies between the antennas. Variations are attributed to the mobility of body parts (e.g., hands, torso, head, etc), as is practically impossible for a body to remain completely static. Five realization sets have been obtained in the second category. We observe in Fig. 3 rapid power fluctuations when human shadowing occurs, together with a sharp reduction of power during this time interval (that is the ERTI T_e in each realization). The utilization of highly directional antennas further enhances this effect, as the link switches abruptly from a "good state" (i.e., unobstructed link) to a "bad state" (i.e., obstructed link). The majority of attenuations are between *5-20dB* in the first category, lasting for about *6sec*. As was expected, the majority of attenuations in the second category are much higher, i.e., between *45-65dB*.

From the preceding statistical analysis and the above discussion about the measurement categories in Fig. 3, it is clear that the received power levels in each category will follow a Gaussian probability distribution. This is evident from Fig. 4, where the probability distributions of measured power levels in each category are shown. The mean value and standard deviation for the collected power levels in the first category (i.e., shadowing due to slow mobility of humans) are *-13.2 dB* and *3.9 dB*, respectively. In the second category (shadowing due to static human bodies), the mean value and standard deviation are *-55.1 dB* and *7.9 dB*, respectively. In this figure, we also present the respective Gaussian probability distributions with the aforementioned mean values and standard deviations for each category. The correlation coefficients [18] between the measured and theoretically predicted power levels are *0.985* and *0.986* for the first and second shadowing process, respectively, showing a very good statistical compliance. Thus, the distribution of the measured power levels for both shadowing processes is satisfactorily approximated by a Gaussian distribution.

IV. Conclusion

Received power measurements have been collected in the *60GHz* band under the presence of human activity between the antennas in short-range indoor links. Two different, but very commonly encountered, shadowing processes were considered. Very abrupt power fades were observed due to human body shadowing. We have shown that received power fluctuations arisen from the same shadowing process are adequately modeled by a Gaussian distribution. Such a result is also compatible with a theoretical statistical analysis based on an additive model. As our theoretical analysis upgrades an existing powerful theory in [10], it is valid for any frequency of operation, type and number of scatterers, antenna patterns and polarization. Our approach can be very useful for current and future developments in IEEE 802.15.3c and IEEE 802.11ad standards.

[1] A proof can be seen in [17, pp. (98)] for space and frequency varying channels written in the form of [17, eq. (4.4.1)]. A similar proof can be derived for time varying channels written in the form of equation (2).

[2] A proof can be seen in [17, pp. (111)] for space and frequency varying channels. A similar result was presented in [10] for space varying channels. A similar proof can be derived for time varying channels (equation (2)), leading to equation (3).

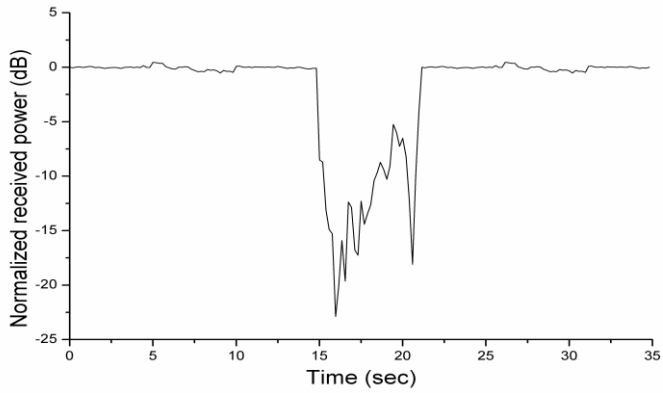

A)

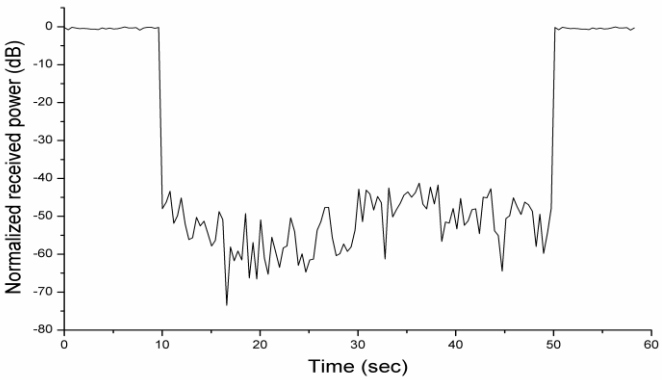

B)

Fig. 3. Examples of measured normalized time-domain received power. A) Mobility of two people. B) Static body.

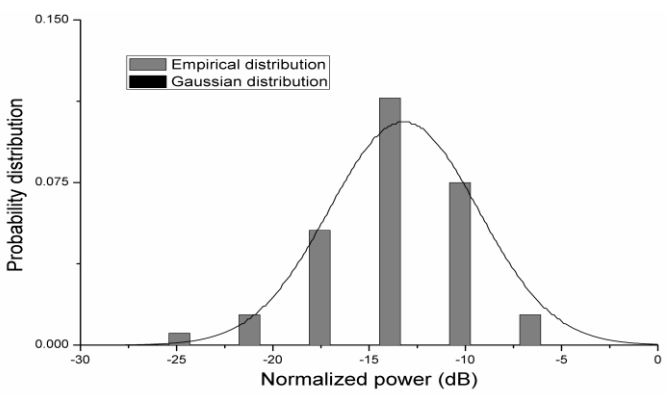

A)

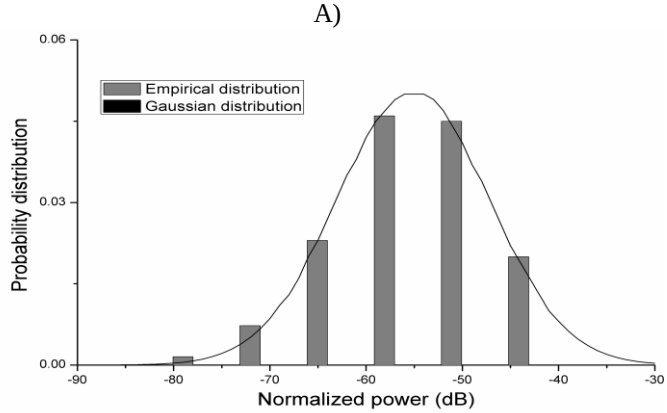

B)

Fig. 4. Probability distributions of measured power levels and Gaussian distributions. A) Mobility of two people. B) Static body.

ACKNOWLEDGMENT

The authors would like to thank Dr. P. McCluskey from Rohde & Schwarz for his help and suggestions in calibrating the measurement equipment. The authors are also grateful to Dr. E. Okon for his useful discussions during the preparation of this work.

REFERENCES

[1] T. S. Rappaport, J. N. Murdock and F. Gutierrez, "State of the Art in 60-GHz Integrated Circuits and Systems for Wireless Communications," Proc. IEEE, vol. 99, no. 8, pp. 1390-1436, Aug. 2011.

[2] IEEE 802.15 WPAN Millimeter Wave Alternative PHY Task Group 3c (TG3c), online: http://www.ieee802.org/15/pub/TG3c.html.

[3] E. Perahia C. Cordeiro, M. Park and L. L. Yang, "IEEE 802.11ad: Defining the Next Generation Multi-Gbps Wi-Fi," IEEE Cons. Commun. Netw. Conf. (CCNC), pp. 1-5, Jan. 2010.

[4] S. Collonge and G. Zaharia, "Influence of the Human Activity on Wide-Band Characteristics of the 60 GHz Indoor Radio Channel," IEEE Trans. Wirel. Commun., vol. 3, no. 6, pp. 2396-2406, Nov. 2004.

[5] S. Obayashi and J. Zander, "A Body-Shadowing Model for Indoor Radio Communication Environments" IEEE Trans. Ant. Propagat., vol. 46, no. 6, pp. 920-927, Jun. 1998.

[6] P. Karadimas, B. Allen and E. Okon, "60 GHz Time-Domain Propagation Measurement System," Loughborough Ant. Propagat. Conf. (LAPC), Nov. 2012.

[7] J. Wang, R. V. Prasad and I. Niemegeers, "Analyzing 60 GHz Radio Links for Indoor Communications" IEEE Trans. Cons. Electr., vol. 55, no. 4, pp. 1832-1840, Nov. 2009.

[8] M. Jacob, S. Priebe, A. Maltsev, A. Lomayev, V. Erceg and T. Kurner, "A Ray Tracing Based Stochastic Human Blockage Model for the IEEE 802.11 ad 60 GHz Channel Model," Eur. Conf. Ant. Propagat. (EUCAP), pp. 3084-3088, Apr. 2011.

[9] T. Manabe, Y. Miura and T. Ihara, "Effects of Antenna Directivity and Polarization on Indoor Multipath Propagation Characteristics at 60 GHz," IEEE Journal Selec. Areas Commun, vol. 14, no. 3, pp. 441-448, Apr. 1996.

[10] J. Salo, L. Vuokko, H. M. El-Sallabi, and P. Vainikainen, "An Additive Model as a Physical Basis for Shadow Fading," IEEE Trans. Veh. Technol., vol. 56, no. 1, pp. 13–26, Jan. 2007.

[11] P. F. M. Smulders, "Statistical Characterization of 60 GHz Indoor Radio Channels," IEEE Trans. Ant. Propagat., vol. 57, no. 10, pp. 2820-2829, Oct. 2009.

[12] Z. Genc, W. Van Thillo, A. Bourdoux and E. Onur, "60 GHz PHY Performance Evaluation with 3D Ray Tracing under Human Shadowing," IEEE Wirel. Commun., Lett., vol. 1, no. 2, pp. 117-120, Apr. 2012.

[13] M. Park and H. K. Pan, "A Spatial Diversity Technique for IEEE 802.11ad WLAN in 60 GHz Band," IEEE Commun., Lett., vol. 16, no. 8, pp. 1260-1262, Aug. 2012.

[14] V60WGD02 60 GHz Waveguide Development System, online: http://www.vubiq.com/prod_waveguide_dev.php.

[15] B. H. Fleury, "First- and Second-Order Characterization of Direction Dispersion and Space Selectivity in the Radio Channel," IEEE Trans. Inf. Theory, vol. 46, no. 6, pp. 2027-2044, Sep. 2000.

[16] J. B. Andersen, J. Ø. Nielsen, G. F. Pedersen, G. Bauch and G. Dietl, "Doppler Spectrum from Moving Scatterers in a Random Environment," IEEE Trans. Wirel. Commun., vol. 8, no. 6, pp. 3270-3277, Jun. 2009.

[17] G. D. Durgin, "Space-Time Wireless Channels," Prentice Hall, 2003.

[18] A. Papoulis and S. U. Pillai, "Probability, Random Variables and Stochastic Processes-4th ed.," McGraw–Hill, 2002.